INSTITUTE OF PHYSICS PUBLISHING JOURNAL OF PHYSICS: CONDENSED MATTER

J. Phys.: Condens. Matter **14** (2002) 1–16 PII: S0953-8984(02)34075-X

Raman scattering and quantum confinement in heavily electron-irradiated alkali halides

E I Shtyrkov[1], A Klimovitskii[2], H W den Hartog[3,4] and D I Vainshtein[3]

[1] Kazan Physical-Technical Institute, AS of Russia, 420029 Kazan, Russia
[2] Kazan State University, 420000 Kazan, Russia
[3] Solid State Physics Laboratory, University of Groningen, Nijenborgh 4, 9747 AG Groningen, The Netherlands

E-mail: h.w.den.hartog@phys.rug.nl

Received 21 February 2002, in final form 16 May 2002
Published
Online at stacks.iop.org/JPhysCM/14/1

Abstract

In this paper we will study the properties of several unusual Raman scattering peaks in heavily irradiated NaCl with vast amounts of colloidal sodium and chlorine precipitates. It appears that the laser excitation light interacts with both the electronic and vibration systems of the Na colloids, which gives rise to new Raman scattering peaks, which can be associated with electronic and vibrational excitations confined in extremely thin (about 6 nm) quantum wires.

1. Introduction

The great interest in nano-size materials is due to their very unusual properties, which are often quite different from those of bulk samples. Their properties stem from the confinement of electrons/holes or phonons in small volumes [1]. Interactions between confined electrons or phonons with their environment lead to a wealth of optical properties and processes, for instance, strong photoluminescence [2, 3] and electroluminescence [4] of quantum wires in porous Si in the visible region of the optical spectrum, quantization of the electronic motion in transport measurements (quantum Hall effect [5]), enhanced third-order nonlinear optical susceptibility, as observed in silicate glass with dispersed colloidal Au particles [6], and a number of nonlinear optical effects in quantum confined structures [7]. It is interesting to study the physical properties of systems with sizes comparable with the characteristic quantum mechanical length scale determined by the coherence of the wavefunctions. Some examples such as quantum wires, systems with quasi-zero-dimensional quantum dots [8], and two-dimensional heterostructures of semiconductors [9], have been investigated with a number of optical techniques [10] including luminescence and Raman spectroscopy (RS). RS has been applied successfully to metal and semiconductor nano-clusters and particles in glasses and crystals [11, 12].

[4] Author to whom any correspondence should be addressed.

RS of doped, additively and electrolytically coloured NaCl crystals have revealed alterations in the spectra of inelastic light scattering at low frequencies, i.e. below the phonon cut-off frequency of NaCl, due to the presence of small-sized metallic nano-particles [13, 14]. Strong alterations in the Raman spectra and the appearance two new peaks beyond the range of the one-phonon excitations of NaCl were discovered in doped, heavily irradiated rock salt [15]. These peaks were interpreted as the result of strong radiation damage in the crystals but their origin is still unclear. It was concluded that the peaks are associated with ultrafine details of the small particles that are present in heavily irradiated samples, and which have been detected by differential scanning calorimetry experiments [16]. As was established with electron spin and nuclear magnetic resonance, as a result of the exposure to ionizing radiation, simple, colloid structures in doped NaCl can be transformed into thin wires consisting of colloidal Na [17], which might possess the quantum properties of a one-dimensional degenerate electron gas (1DEG).

With the aim of learning more about the origin of inelastic light scattering in these materials, we have studied in this work in detail the Raman spectra of heavily damaged NaCl:KBF_4 and NaCl:K crystals with different irradiation doses, as a function of the wavelength, the polarization condition of the excitation light, and the measuring temperature.

2. Experiments and results

Raman scattering experiments have been carried out in the conventional 90° geometry as a function of the temperature (30–200 K). The spectra were excited by means of 488 and 514.5 nm light of a Spectra Physics model 171 argon-ion gas laser (100 mW) and recorded with a spectrometer equipped with a SPEX 14018 double monochromator coupled with a cooled EMI 9826A Photo Multiplier Tube (PMT). The slits of the monochromator were 250 μm, resulting in a resolution of 3.0 cm^{-1}. The pulses, produced by the photomultiplier, were counted by a DPC 2 pulse counter. The counts were registered by a Nucleus 2048 MCA in a personal computer.

We have measured the polarized and depolarized spectra with $X(ZZ)Y$ and $X(ZX)Y$ geometries (X is the direction of the laser beam, and Y is the direction of observation). For the measurements at low temperatures (as low as 30 K) the samples were glued onto a copper sample holder, which is located in a cryostat with optical quartz windows. Additional measures were taken to reduce the effects of light scattering by the sample holder on the spectra.

The (doped) NaCl single crystals have been prepared in our crystal growth facility by means of a Bridgman set-up. Details of this set-up have been described elsewhere [18]. The samples with a thickness of up to 1.0 mm used for this investigation were cut from the cylindrical boules with a diameter of 6 mm using a 'chemical saw' device with a thin cotton wire, which was saturated with alcohol. After cutting the samples they were polished until they showed a shiny surface.

The irradiation runs were carried out with an electron accelerator. We have used two sample types, which show the same properties. The first group of samples were irradiated with 1.35 MeV electrons, while the second group were exposed to 0.5 MeV electrons. Due to the reduced penetration of the 0.5 MeV electrons, we have used for these experiments samples with thickness up to 0.5 mm.

The sample holder used in our irradiation facility has more than 300 locations where a sample can be accommodated. All samples are irradiated simultaneously at the same dose rate. The sample holder consists of 15 sub-targets, which can be kept at different fixed temperatures between 50 and 150 °C.

The samples can be characterized conveniently by means of differential scanning calorimetry (DSC) experiments, where the melting peaks of radiolytic Na are measured. The melting

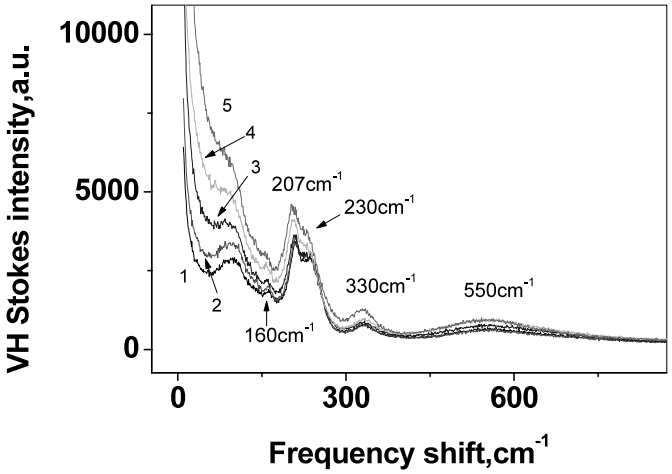

Figure 1. The Raman VH spectra of heavily electron irradiated crystal NaCl:K (sample 2, $T_{irr} = 110\,^{\circ}$C, 150 grad with 3.6 mol% Na); the measuring temperatures are: 1: 30; 2: 50; 3: 100; 4: 150; 5: 200 K.

Table 1. The irradiated NaCl:X samples used in this investigation.

Sample number	Impurity (mol%)	Irradiation T (°C)	Irradiation dose (grad)	Concentration of Na colloids (mol%)
1	K (0.1)	100	150	2.9
2	K (0.1)	110	150	3.6
3	K (0.1)	120	150	2.7
4	KBF_4 (300 ppm)	140	150	5.7
5	KBF_4 (300 ppm)	90	150	7.9

phenomena associated with colloidal Na are observed in the vicinity of 100 °C. The concentration of Na is determined by using the literature value of the specific heat of melting of Na metal. The Na concentrations in the samples used in this investigation are given in table 1.

The measuring temperature during the Raman scattering experiments was determined with an accuracy of 1 K. The Raman spectra were taken at different temperatures in the range 30–200 K.

A few of the typical inelastic scattering spectra for heavily electron irradiated NaCl:X crystals taken at different temperatures are shown in figure 1.

In the range up to 300 cm^{-1} we have observed a continuous Raman spectrum, which is, depending on the sample and measuring temperature, superimposed upon by strong Raman peaks (160, 207, 230 cm^{-1}). Most of these lines have been obtained earlier for both additively and electrolytically coloured rock salt [13, 14]. Increasing the sample temperature during the measurement results in a strong broadening of the Rayleigh line to mask the Stokes intensity for all frequencies below 100 cm^{-1} due to the well-known factor [19] for first-order scattering

$$R_{s1}^{(1)} = (\bar{n} + 1),$$

where the Bose–Einstein coefficient is defined as $\bar{n}(\nu, T) = (e^{\frac{h\nu}{kT}} - 1)^{-1}$, and ν is the phonon vibration frequency. Therefore, in order to eliminate these temperature effects on the phonon spectrum in question (for frequencies close to zero), we reduced the spectra by dividing the RS intensity by a factor $R_s^{(1)}$ and the resulting spectra are presented in figure 2.

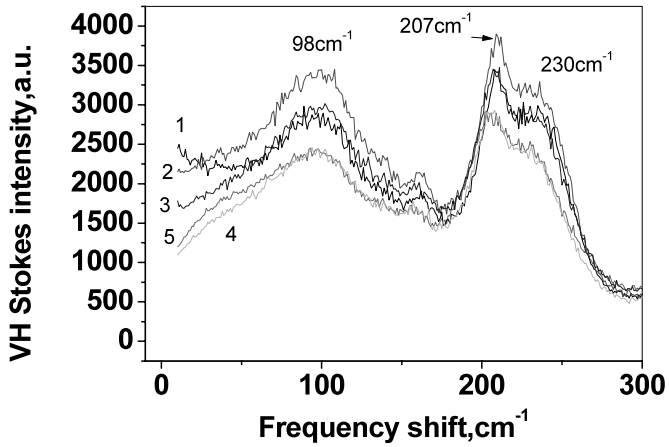

Figure 2. Reduced low-frequency RS intensity for sample 2; the measuring temperatures are: 1: 30; 2: 50; 3: 100; 4: 150; 5: 200 K.

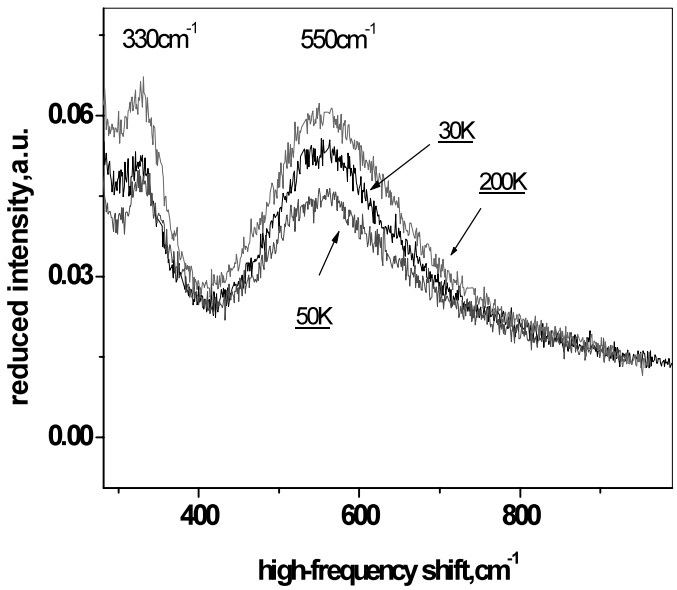

Figure 3. The high-frequency Stokes Raman spectra for NaCl:KBF_4 (sample 4, with 5.7 mol% Na) measured at 30, 50, and 200 K.

In contrast to the results in figure 1, we see in figure 2 that in the low-frequency region (below 60 cm^{-1} the intensity of the inelastic scattering decreases with increasing temperature. In contrast with this behaviour, the other RS lines increase rather smoothly in intensity with increasing temperature, as expected for phonon peaks.

The other important point to emphasize with regard to the Raman spectra of heavily electron irradiated alkali halides is the appearance of two rather strong peaks at 330 and 550 cm^{-1} beyond the cut-off frequency of the one-phonon spectra of the host crystal, which were first reported in [15]. These additional lines (figure 3) have a rather smooth shape.

On the other hand the shape of the peaks shows some differences. The main features of the second extra peak (at 550 cm^{-1}) are the very large width of the line and the long tail, which

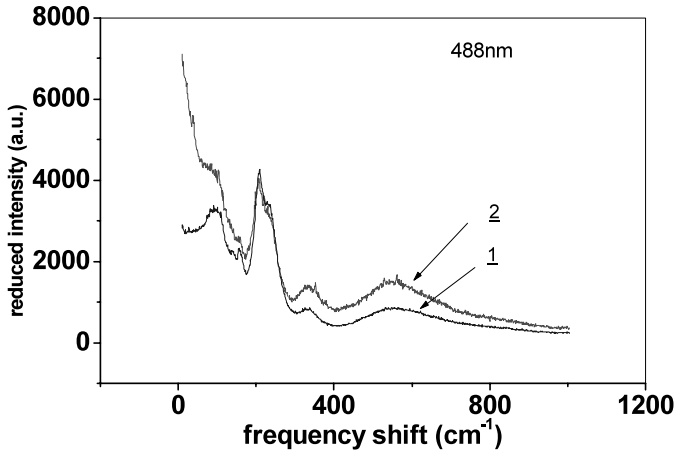

Figure 4. RS spectra for samples with different concentrations of Na colloids taken at 150 K: 1: sample 1 (2.9 mol% Na); 2: sample 4 (5.7 mol% Na).

extends up to 1000 cm^{-1}. Also, both peaks consist of several contributions from individual lines giving rise to the overall appearance due to averaging over the intensity distribution.

In the low-frequency part of the spectrum (for frequency shifts less than 50 cm^{-1}) the inelastic scattering intensities increase with increasing doses due to the presence of increased concentrations of defects. This behaviour has been reproduced several times. The same behaviour is observed for the peaks beyond the cut-off frequency (see the reduced spectra in figure 4). At the same time the other peaks (160, 207, 230 cm^{-1}) show a weak dependence on the concentration of the Na nano-particles.

We have investigated the changes in the peak position as well as the changes in the band shapes as a function of the temperature. The peak positions of the above-mentioned lines at 330–550 cm^{-1} are almost independent of the temperature, which is quite unusual for Raman scattering peaks. According to [20, 22] the frequency position of the RS lines should decrease with increasing temperature. As can be seen in table 2, where the peak positions at temperatures between 30 up to 200 K are given for the samples investigated in this paper, the downward shift is usually about 4–5 cm^{-1} for the peaks at 160 and 207 cm^{-1}. Table 2 shows that the line at about 330 cm^{-1} reveals a deviating behaviour. This is also the case for the wide 550 cm^{-1} band.

The effect of the frequency shift for the lines at 160 and 207 cm^{-1}, showing the normal behaviour, is obviously due to changes of the quasi-elastic constant of the crystal, because decreasing temperatures result in a compression of the volume and, accordingly, to confinement of the phonons with smaller wavelengths. It is clear that the 330 and the 550 cm^{-1} peaks do not show the same behaviour.

We have found that for small wavenumbers ($<100\ cm^{-1}$) the polarization ratio (VH/VV) of the scattered light decreases rapidly from 0.5 to 0.2, while this ratio is about 0.75 at frequencies higher 200 cm^{-1}. The behaviour of the depolarized spectra is due to a strong anisotropy of the scattered light (figure 5). It should be emphasized that the polarization ratio shown in figure 5 should be interpreted as an effective spectral coefficient, which coincides with the real polarization ratio of a single RS line only if there is no overlapping with adjacent peaks. Nevertheless, this parameter is also useful to show the qualitative behaviour of the different components of the RS spectra—for instance, the different behaviours of the polarization ratio

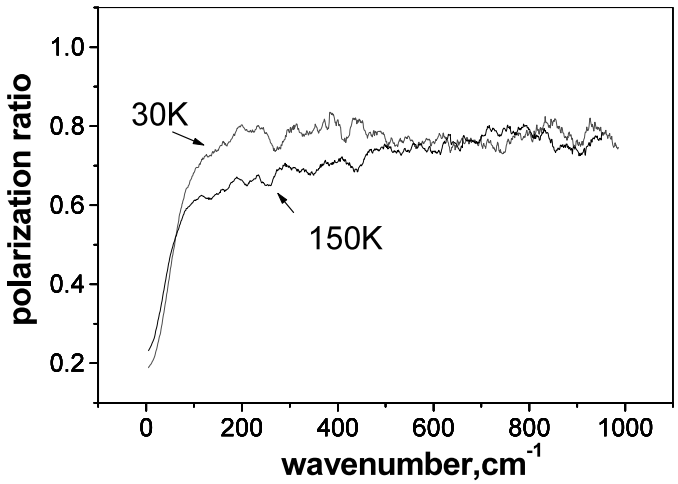

Figure 5. The dependence of the RS depolarization ratio as a function of the frequency for sample 4, NaCl:KBF_4 (5.7 mol% Na).

Table 2. Raman peak positions versus T for some scattering peaks.

Sample type Excitation wavelength Colloid concentration	T (K)	Frequency shift position (cm^{-1})		
Sample 1	30	161	206	322
NaCl:0.1% K	50	160	205	328
488 nm	100	159	204	323
2.9% Na, LH = 1.45 J g^{-1}	150	157	203	324
	200	157	201	321
Sample 2	30	161	209	329
NaCl:0.1% K	50	162	210	331
488 nm	100	160	208	330
3.6% Na, LH = 1.85 J g^{-1}	150	159	206	330
	200	157	205	327
Sample 3	30	161	209	326
NaCl:0.1% K	50	160	209	328
488 nm	77	158	208	330
2.7% Na, LH = 1.37 J g^{-1}	100	159	206	332
	150	157	206	328
	200	156	204	324
Sample 4	30	159	210	323
NaCl:300 ppm KBF_4	50	160	209	323
488 nm	77	159	208	324
5.7% Na, LH = 2.85 J g^{-1}	100	160	208	324
	150	158	206	331
	200	155	204	325
Sample 5	30	161	209	328
NaCl:300 ppm KBF_4	50	161	209	327
488 nm	77	160	208	330
7.9% Na, LH = 4.02 J g^{-1}				

for energies below and higher then 100 cm^{-1}, which has been observed for several samples and in a wide range of temperatures.

It can also be seen from figure 5 that in the frequency range below 50 cm^{-1} the behaviours of the polarization factor are similar for different measuring temperatures. Similar values for the depolarization ratio (like in our case, close to 0.3 for frequencies less than 50 cm^{-1}) were obtained for silver particles in silica [23] and for silver particles in alkali halides [11]. For the latter system the observed depolarization ratios of 0.27 were assigned to quadrupolar spheroidal mode vibrations with $l = 2$, which are the only Raman-active modes [24] in the zero-wavenumber region. Our results suggest that in heavily irradiated samples nano-particles with wide distributions of shapes and sizes exist, especially in the NaCl:KBF_4 samples, which are affected the most by ionizing radiation.

3. Discussion

3.1. The low-frequency region (10–300 cm^{-1})

Because alkali halide crystals show a high degree of translation and many elements of mirror and axial symmetry, all optical phonon excitations of the first-order spectrum of pure NaCl are missing [19]. Therefore, one usually observes in NaCl exclusively the weak second-order RS excitations produced by inelastic scattering [25, 26]. A clear confirmation of the dominant two-phonon scattering process in pure rock salt is that the full width of the RS spectrum is approximately a factor of two wider than the maximum frequency of the spectrum of the elastic vibrations of rock salt, where four fundamental modes are found at $\nu_1 = 101$ cm^{-1} (TA mode), $\nu_2 = 151$ cm^{-1} (TO), $\nu_3 = 159$ cm^{-1} (LA), and $\nu_4 = 217$ cm^{-1} (LO) calculated in [27].

In doped NaCl (additively and electrolytically coloured NaCl [13]), second-order RS scattering has also been observed in the low-frequency range of the spectra. However, because of the lowering of the crystal symmetry due to defects, stronger first-order lines are observed. The spectrum has a cut-off frequency of about 260 cm^{-1} (figure 1), which is close to the values calculated by Bilz and Kress [28] but smaller than the phonon cut-off frequency for pure NaCl (370 cm^{-1}). This forms the main feature of the RS spectra for NaCl crystal either with defects or in the presence of nano-particles. As a result of the reduced background, several sharp lines [13] at about 80, 100, 115, 134, 154, 205, and 230 cm^{-1}, are observed which appear to be in the close vicinity of the critical points of the normal phonon spectrum of NaCl, which are found at 79, 111, 120, 140–142, 150, 208, 230 cm^{-1} by means of inelastic neutron scattering [29].

See endnote 1

For the continuous RS spectrum below 100 cm^{-1}, and in the case of small correlation lengths, as observed in amorphous media and highly defective crystals, the temperature effect should be eliminated by a reduction method suggested by Shuker and Gammon [30], which consists of dividing the RS intensity by a factor $f = R_s^{(1)}/\nu$. Due to the strong disorder in our heavily irradiated samples, the selection rules for the phonon wavevector partly break down, and one might expect to observe first-order Raman scattering bands. Obviously, we observe this in figure 6 where polarized $X(ZZ)Y$ and depolarized $X(ZX)Y$ spectra have been reduced to show the clearly different temperature behaviour of the scattering intensity for frequency shifts below 60 cm^{-1}.

To evaluate the signal-to-noise level in our experiment we show the peak due to elastic scattering of the nearest plasma line (488.9 nm) excited in the cavity of our laser. The continuous RS spectrum in the low-frequency range, as observed earlier for doped NaCl crystals, suggests that filamentary clusters of metal Na colloids are present. This part of the spectrum is interpreted as a continuous distribution of curvatures of the surface, which is

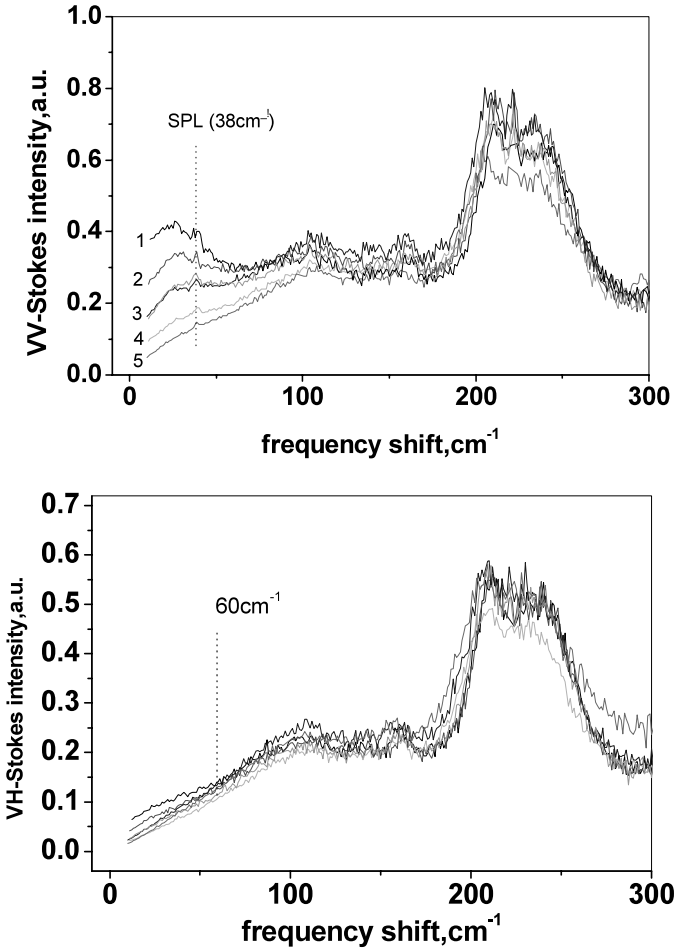

Figure 6. Low-frequency RS for sample 4 (normalized VV and VH Stokes spectra, reduced by factor f); 1: 30; 2: 50; 3: 100; 4: 150; 5: 200 K. SPL-source plasma line (elastic scattering of the laser 488.9033 nm light).

assumed to have a fractal shape [31, 32]. Nano-sized particles have large fractions of surface atoms compared with total numbers of atoms. Therefore surface effects will be very important and most probably they can be revealed conveniently by inelastic light scattering experiments.

In our case the presence of the bands centred around 20 cm^{-1} can be assigned directly to scattering by phonons localized on dendrite-like nano-structures of metallic Na (small-sized filamentary sodium nano-particles). In the low-frequency region of the RS spectrum (below 60 cm^{-1}) this band has a width of about 10–40 cm^{-1}. As a result of the localization of the phonons (phonon confinement) within these wires there is a discrete set of vibrational modes for a free wire. However, when this wire is not free and when it is embedded in an elastic matrix, the discrete set broadens into a continuum [32]. This might be the explanation for the large width of the above-mentioned peak. To evaluate roughly the mean thickness of the wire, the relation between the typical size of the nano-particles d and the frequency shift—in the

case of free boundary conditions—can be used [32]:

$$\nu_p \ (\mathrm{cm}^{-1}) = \frac{V q_p}{2\pi c}, \qquad q_p = \frac{\pi}{d} p, \ p = 1, 3, 5, \ldots \tag{1}$$

where V and c are the velocities of sound and light, respectively, and q is the modulus of the phonon wavevector. This equation specifies the vibrations having nodes at the colloid surface (standing waves, phonon confinement) and it allows us to estimate the mean size of the colloid. For sodium [33] the longitudinal sound velocity $V = 3.2 \times 10^5$ cm s^{-1} and for $p = 1$ (the inner mode) this equation yields values for the thickness of the wires in the range 1.5–6.0 nm. Alternatively, similarly to the case for semiconductors [34], the presence of the background (between 10 and 100 cm^{-1}) for our heavily irradiated NaCl samples can also be explained by single-particle excitations of the electron gas in metallic nano-particles. However, this idea requires additional investigations of the scattering phenomena in the range near zero frequency (<10 cm^{-1}).

To clarify whether the occurrence of the lines observed at energies higher than 100 cm^{-1} is caused by metal clusters of spherical or filamentary shape, or by scattering due to the host lattice, we have estimated the frequency shifts of these lines as a result of changes in the temperature. We have compared the calculated values for the shifts with experiment (see table 2). We have used the feature that for a spherical object and for a wire, the relative volume changes as a function of the temperature are different. It follows from expression (1) that the relative frequency shift of an elastic wave is related to the dimensional changes in accordance with the relationship

$$\frac{\Delta\nu}{\nu} = -2\frac{\Delta d}{d}.$$

For a wire the relative changes of the thickness are related to the volume changes as

$$\frac{\Delta d}{d} = \frac{\Delta V}{2V}.$$

The corresponding relation for a sphere (with d the diameter) is

$$\frac{\Delta d}{d} = \frac{\Delta V}{3V}.$$

The mean coefficient of volume expansion is equal to

$$\beta = -\frac{1}{\Delta T}\frac{\Delta V}{V}.$$

In the case of spherical objects we find

$$\frac{\Delta\nu}{\nu} = -(\beta/3)\,\Delta T$$

while for a wire we calculate for the frequency shift

$$\frac{\Delta\nu}{\nu} = -(\beta/2)\,\Delta T.$$

For sodium [35] the coefficient of volume expansion is equal to 177.9×10^{-6} °C^{-1} and using this parameter we estimate the relative change of the RS frequencies for $\Delta T = 170$ °C in the case of spherical particles to be 1%, while for a wire the corresponding value is 1.5%. For natural rock salt [36] $\beta = 116.7 \times 10^{-6}$ °C^{-1} and the estimated shifts for spheres and wires are now 0.7 and 1%, respectively.

Our experimental data for the frequency shifts as a function of the temperature observed for the peaks at 161 and 207 cm^{-1} (see table 2) show that the (average) relative change of the frequency is equal to 2.5%, which is rather close to the estimates given above. Unfortunately,

these results do not allow us to make a choice regarding the shape of the nano-particles. On the other hand, for the peaks at 325, 330, and 530 cm^{-1}, showing very small shifts, the relative change of the frequency is considerably smaller than expected theoretically. This means that the above-mentioned considerations are absolutely invalid for these peaks. Apparently, we are dealing here with another, essentially different light scattering mechanism.

3.2. Peaks beyond the cut-off frequency of the phonon spectrum of NaCl

The new RS lines observed in heavily irradiated alkali halide crystals at about 330 and 550 cm^{-1} are located beyond the phonon cut-off frequency of crystalline rock salt. In principle, the scattering peak at 330 cm^{-1} could be interpreted as an overtone of the main peak in the infrared absorption spectrum (TO mode F_{1u}, 162 cm^{-1}). We note that a similar two-phonon phenomenon has been observed in optical absorption experiments, because an absorption maximum at 328 cm^{-1} has been observed earlier [37] at 300 K. Unfortunately, we do not have information on the IR absorption spectra for our samples. Although we think that these two-phonon processes are not linked with the RS line at 330 cm^{-1}, we cannot exclude fully the possibility that this RS peak is due to two-phonon excitations.

As to the second peak, there is a rather plausible mechanism to explain the scattering by molecular chlorine gathered in bubbles. In principle, the peak at 550 cm^{-1} could be explained by first-order scattering due to chlorine molecules (the transition is located at 564 cm^{-1}). Because a Cl_2 molecule has a symmetry centre, this absorption is usually not observed in the IR range. Consequently, it should be active in Raman scattering, because in contrast with the case for IR absorption, this transition will be allowed in Raman scattering. The large width of the line could be associated with the existence of a wide distribution of bubble sizes and a wide range of internal pressures within these precipitates. The distribution of internal pressures could be the reason for the broadening, and the frequency shift might be due to the large variety of individual particles. In fact, we know that during irradiation at moderate temperatures, Na nano-particles are formed together with chlorine precipitates (see [38, 39]). The presence of chlorine can be demonstrated quite easily by crushing heavily irradiated NaCl samples. During this process one can clearly smell the chlorine gas escaping from the irradiated rock-salt sample. In addition, the presence of chlorine has been established by means of latent heat (LH) experiments, showing an endothermal peak at about $-101\,^{\circ}C$ representing the melting peak of chlorine (the triple point of chlorine is located at $-101\,^{\circ}C$). Our results from the radiolysis of NaCl can be explained in the framework of a theoretical model, which has been developed recently by us [40].

The presence of nano-sized chlorine bubbles is quite essential in the radiolytic processes in NaCl, because chlorine bubbles represent one of the driving forces of the damage production in heavily irradiated NaCl. Due to the high pressure (in the gigapascal range) in the bubbles, the transport of the primary F and H centres is biased. Especially in the case of very small bubbles, it is more probable that an H centre arrives at the bubble than an F centre. In heavily irradiated NaCl there are voids and cracks, which are filled with chlorine with pressures of typically 5×10^{-3} GPa (50 bar) [41]. In most samples the amount of chlorine in these voids and cracks is only small as compared to the total amount of radiation-induced chlorine in the sample.

The consequences of the presence of these widely varying chlorine systems for the physical properties depend strongly upon the presence of the very large differences in the pressure. We have observed that up to moderate concentrations of chlorine (0.5–1.0%) the melting peak of Cl_2 is reduced strongly compared with the one expected on the basis of the melting peak of Na. We assume that these differences should be ascribed to the extremely small sizes and very

high pressure within the chlorine precipitates. Similarly, we expect the enormous and varying local pressures to affect the Raman scattering properties very strongly. The overall properties, such as peak position, line shape, and linewidth, of the peak have to vary strongly with the history (e.g. irradiation dose, dose rate, partial annealing) of the sample. However, there are no such enormous variations for RS at about 550 cm^{-1}. Taking this into account, we assume that in our heavily irradiated NaCl samples the 550 cm^{-1} peak is not due to chlorine molecules and that it is caused by excitations localized at the precipitates of the other type, the metallic nano-particles.

Concerning the occurrence of the peaks at 330 and 550 cm^{-1}, it was proposed earlier [16] that these lines might be caused by light scattering of sodium colloids and that they are due to some kind of local excitation. In favour of the explanation in terms of sodium colloids is the fact that in our samples the peaks are not observed for samples with a low dose of electron irradiation and that they increase with increasing dose (see figure 4). In earlier experiments [15] it was shown that these peaks at 330 and 550 cm^{-1} are not observed after annealing of the samples and when the RS spectra are taken at room temperature.

Although the amount of metallic Na appears to be approximately constant, the melting behaviour of the nano-particles has also changed after Raman scattering experiments at room temperature. In the first case the colloids are most probably compact conglomerates of Na metal, i.e. the above-mentioned wire-like structure is not present. In the second situation the additional peaks are not observed due to photon-simulated diffusion resulting from laser excitation of a sample while taking the spectra. The disappearance of only these lines in the spectrum upon thermal annealing confirms this interpretation for the scattering mechanism. It should be noted that the intensity of the other RS lines is conserved upon annealing.

Together with the earlier results supporting the idea of the fractal nature of the colloidal surface, our present observations reveal the presence of nano-sized metallic precipitates with dendrite-like geometry. In such systems, quantum size effects are expected, which originate from the mechanism of quantum confinement of the electron gas in narrow local potential wells and wires. Quantum confinement effects are observed for systems with sizes which are comparable with the characteristic quantum mechanical length scale, which defines the coherence of the electronic wavefunction. As the numbers of conduction electrons in small particles are small (for example a particle with a diameter of 10 nm contains approximately 10^4 electrons), the electrons depend on each other in the 1DEG of nano-sized wires and their energy spectrum is quantized. In other words, small-sized colloids behave analogously to multi-electronic atoms with discrete energy structures, which can give rise to inelastic light scattering. Thus RS scattering allows us to study elementary excitations, which cannot be investigated by luminescence or optical absorption spectroscopy. The reason for this is that the comparison of experiment with the single-particle polarization theory or with the absorption constant in the far-infrared region is difficult, because the quantum effects are masked as a result of the group-wise clustering of the precipitates in heavily irradiated NaCl.

In the model of quantum confinement, inelastic scattering allows us to find the upward energy shift of the peaks associated with electrons, which are confined to a narrow potential well. Thus the kinetics of the light scattering process is determined by the conservation of energy and impulse during the event. We assume that the selection rules for the wavevector associated with Raman scattering are lifted to some extent due to the presence of large amounts of defects in our heavily irradiated samples. The intense and collective interactions during inelastic light scattering events result in an enhancement of the scattered light intensity. These processes are induced in our one-dimensional systems because of the breakdown of the wavevector conservation rule, which is caused by the presence of the radiation-induced defects. Finally, we note that the size distribution of the nano-particles leads to averaging of the

behaviour of an individual particle over the size and shape distribution functions for all particles present, which provides an explanation of the composite shape of lines at 330 and 550 cm^{-1}.

In the case of one-dimensional nano-structures (quantum wires along the z-direction), the motion of the electron gas is restricted to two directions (x, y). The behaviour of confined electrons in these systems (1DEG) can be described by a rectangular cylindrical potential well, for which the Schrödinger equation for a two-dimensional energy potential $U(x, y)$ is

$$-\frac{\hbar^2}{2m^*}\left[\frac{\mathrm{d}^2}{\mathrm{d}x^2}+\frac{\mathrm{d}^2}{\mathrm{d}y^2}+\frac{\mathrm{d}^2}{\mathrm{d}z^2}\right]\psi + U(x, y)\psi = E\psi. \tag{2}$$

Here, the m^* is the effective mass of the electron, E is the energy, and the potential energy function U is assumed to have cylindrical symmetry:

$$U(x, y) = U(\rho) = \begin{cases} -U_0 & \text{for } \rho \leqslant \rho_0 \\ 0 & \text{for } \rho \geqslant \rho_0 \end{cases}$$

where radius of the wire $\rho_0 = d/2$.

The depth of the potential well U_0 depends on the energy difference between the Fermi level close to the surface of the nano-particle and the bottom of the conduction band of the NaCl matrix, and the work function of Na metal. In our case U_0 is several electron volts, i.e. the requirement of an infinitely deep potential well is fulfilled. For this situation the eigenfunctions of the electron and hole, obtained by solving equation (2), are [42]

$$\Psi_{m,n,p_z} = a\left[J_m\left(j_{m,n}\frac{\rho}{\rho_0}\right)\Big/ J_{m+1}(j_{m,n})\right]\exp(\mathrm{i}\varphi)\exp(\mathrm{i}p_z z/\hbar) \tag{3}$$

where J_m is the Bessel function of mth order, and $j_{m,n}$ is its nth root.

From the requirement of continuity of the eigenfunction, it should be equal to zero at the interface, resulting in quantization of the energy levels, and the spectrum of energy eigenvalues is

$$E_{m,n,p_z} = \frac{\hbar^2 j_{m,n}^2}{2m^*\rho_0^2} + \frac{p_z^2}{2m^*}. \tag{4}$$

If the diameter of the nano-channel varies slowly compared with the electronic wavelength, the adiabatic approach can be used and it is possible to apply (4) with $\rho_0 = \rho_0(z)$.

The frequencies associated with transitions between the neighbouring energy levels ($\Delta n = 1$) for $m = 0$, expressed in wavenumbers, can be written as

$$\nu_n\ (\mathrm{cm}^{-1}) = 1230\frac{(j_{0,n+1}^2 - j_{0,n}^2)}{qd^2}, \tag{5}$$

where q is the ratio of the effective mass and the mass of the free electron, and the diameter of a wire d is given here in nanometres.

Taking into account the fact that for sodium $q = 1.24$, it is now possible to estimate the size of nano-particles using equation (5). For $n = 1$ the two first roots of the Bessel function are equal to 2.4 and 5.52 and, accordingly, we estimate (using the peak positions 330 and 550 cm^{-1}), for the most probable diameter for the quantum wire, values of 8.6 and 6.7 nm, respectively.

These values are slightly larger than the sizes evaluated from the phonon localization at low frequencies. The experimental results can also be explained on the basis of the presence of different types of colloid. In this case it is possible to assume that, as a result of the exposure of NaCl + KBF_4 to high-energy electrons, two different types of colloid are formed. The larger width of the second line (at 550 cm^{-1}) could be due to a wider distribution of particle sizes, and

the asymmetry of the line (in particular observed for the high-frequency tail) can be explained by a preference of these samples to form more and smaller particles during irradiation.

The large variation in the geometry of the nano-particles leads to a wide distribution of the electronic energy level spacings. This distribution can be related directly to the size distribution if the shapes of the nano-particles remain approximately the same. The existence of a distribution of wire diameters results in a deformation of the RS peak. Taking this into account, we have considered the influence of the size distribution of the nano-particles with confined electrons to explain the shape of the spectra in the range of high frequencies, using the approach developed by John and Singh [43] for quantum columns in porous silicon. Since the formation of these wires is a stochastic process, we can assume the wires to have a Gaussian distribution of diameter d centred around a mean value with a variance σ:

$$P(d) = \frac{1}{\sqrt{2\pi}\sigma} \exp\left[-\frac{(d-d_0)^2}{2\sigma^2}\right]. \tag{6}$$

Also—in the case of a wire with thickness d—the number of electrons participating in the scattering process is proportional to d^2. Therefore we can write for the probability distribution of the electrons involved in the scattering process

$$P(d) = \frac{1}{\sqrt{2\pi}\sigma} N d^2 \exp\left[-\frac{(d-d_0)^2}{2\sigma^2}\right], \tag{7}$$

where N is a normalization constant. The scattering frequency is related to the diameter of the wire by equation (5). Using the standard procedure (see also [44]), it is possible to find the corresponding frequency distribution:

$$P(\nu) = \frac{1}{2\sqrt{2\pi}\sigma} \frac{N}{\nu}\left[\frac{a}{\nu}\right]^{3/2} \exp\left[-\frac{1}{2}\left(\frac{d_0}{\sigma}\right)^2\left(\sqrt{\frac{\nu_0}{\nu}}-1\right)^2\right]. \tag{8}$$

For sodium we use $a = 2.45 \times 10^4$ cm^{-1} nm^2, and frequency $\nu_0 = a/d_0^2$.

This expression leads to an asymmetric curve and a shoulder at high frequencies, which have actually been observed in connection with our 550 cm^{-1} peak (figure 2). See endnote 2

The distribution of wire diameters causes a downward shift of the frequency as compared to the expected mean peak position. The frequency ν_0, related to the central value of the size distribution, does not coincide with the maximum of the curve representing the scattered light intensity $\nu_{\max}$, which can be calculated theoretically. By deriving the latter frequency using equation (8) and fitting the theoretical results to our experimental curves, we have found the upward shift of the energy of the RS peak due to electron confinement. Because the frequency ν_0, which corresponds with the maximum of the size distribution, is higher than 550 cm^{-1}, the mean value of the wire diameter should be less than the one evaluated earlier (6.7 nm) where the size distribution has not been taken into account.

In fact, taking the derivative of (8) with respect to frequency and using a modification of equation (5) of the form

$$\nu_0 = \frac{a}{d_0^2},$$

we find the following equation for the frequency where the RS peak shows its maximum intensity:

$$\frac{a\nu_0}{\sigma^2}\left[\sqrt{\frac{\nu_0}{\nu_{\max}}}-1\right]\sqrt{\frac{\nu_0}{\nu_{\max}}} = 5. \tag{9}$$

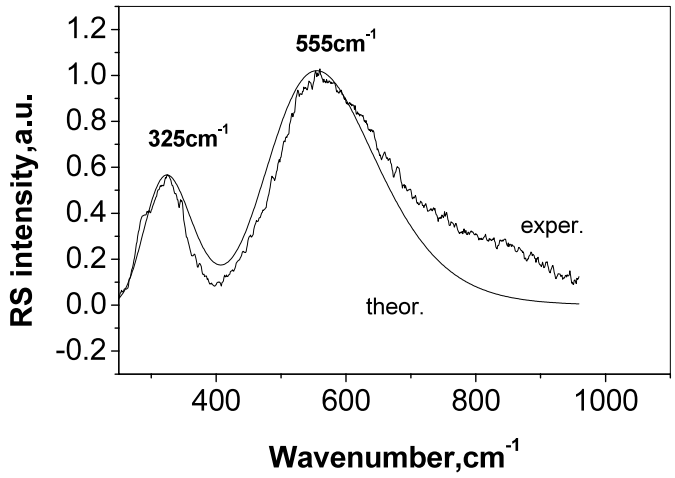

Figure 7. Comparison of the experimental and theoretical RS spectra for NaCl:KBF_4 (5.7% Na). The theoretical spectra were obtained using $\sigma = 0.5$ nm, $d_0 = 6.5$ nm, resulting in $\nu_0 = 582$ cm^{-1} (for the $\nu_{max} = 550$ cm^{-1} peak). For the $\nu_{max} = 325$ cm^{-1} peak we obtain $d_0 = 8.5$ nm, and $\nu_0 = 335$ cm^{-1}; the experimental curve was normalized and this was followed by a baseline subtraction.

From this equation it then immediately follows that

$$\frac{\nu_0}{\nu_{max}} = \left[1 - \frac{5\sigma^2 \nu_{max}}{a}\right]^{-2}. \tag{10}$$

For small values of σ the resulting shape of the RS peak is approximately Gaussian with $\nu_0 = \nu_{max}$. For a normal distribution the variance σ is limited to the range $0 < \sigma < d_0$. For this case the maximum shift can be found by using equation (10) with the condition $\sigma = d_0 = \sqrt{a/\nu_0}$. According to these calculations we find the following relation for the shift range of the Raman scattering peak:

$$1 \leqslant \nu_0/\nu_{max} < 8. \tag{11}$$

In our case $\nu_{max} = 550$ cm^{-1} and the corresponding mean thickness of a quantum wire will be in the range 2–7 nm. This result is close to that evaluated earlier from the phonon confinement concept, which has been applied to explain the Raman scattering bands observed in the range of small wavenumbers. In figure 5 we compare the theoretical curves for the 330 and 550 cm^{-1} peaks, as calculated using equations (8) and (10) and a variance of 0.5 nm, with the experimental spectrum.

From calculations with different values for the variance we have found that improved agreement between the experimental and calculated RS plots can be obtained for this sample. Using a double-Gaussian size distribution of the Na nano-particles with a variance of $\sigma = 0.5$ nm and central values $d_0 = 6.5$ and 8.5 nm, we obtain the results presented in figure 7. These two values for the wire diameter can be ascribed to two different groups of colloids, and the slight difference between the experimental and theoretical curve (e.g. the shoulder at high frequencies) appears to be due to the presence of additional groups of nano-particles with different size distributions.

4. Summary and conclusions

We have observed new scattering phenomena in heavily irradiated rock-salt samples, containing up to almost 8% radiolytic Na and Cl_2. Some of the important characteristic properties have been ascribed to the presence of vast numbers of radiation-induced defects. Transitions which would be forbidden in the perfect NaCl lattice may be partly allowed as a result of the presence of radiation damage. This lifting of the selection rules is important for NaCl, because most of the transitions are not Raman active under normal conditions.

In our heavily irradiated NaCl samples, besides the usual spectra, associated with first- and second-order excitation of NaCl lattice phonons, bands are observed which were ascribed to metallic sodium. In fact, we have observed several Raman scattering peaks for heavily irradiated NaCl in the vicinity of the critical points of the phonon spectrum of sodium which had been determined independently earlier by means of inelastic neutron scattering. This observation confirms that there is a strong interaction between the laser excitation light and the vibrational states of Na nano-particles. The bands around 20 cm^{-1} have been interpreted in terms of excitations of quantum confined vibrational states in the Na nano-particles systems in heavily irradiated NaCl. The width of the peaks is ascribed to the fact that the colloids are embedded in the NaCl crystal lattice. The above-mentioned peaks can be explained in terms of phonon localization in quantum wires with a size between 1.5 and 6.0 nm.

Interaction of laser light with the wire-type nano-sized conglomerates of metallic Na, which are embedded in the NaCl crystal, could also be the reason for the appearance of RS lines due to excitations of the quantum confined system of conduction electrons. We have explained the Raman scattering peaks at 330 and 550 cm^{-1}, which are located beyond the limits of the one-phonon spectrum of NaCl, in terms of electron quantum confinement in nano-wires. Comparison of our experimental results with theoretical calculations taking into account the distribution of sizes have shown that the RS peaks can be explained by excitations of electrons in quantum wires with a mean size of about 6 nm.

At this moment we cannot fully exclude the possibility that there may be other ways to explain the above-mentioned peaks, which are supposed to be due to quantum confined excitations of nano-sized structures in heavily irradiated NaCl. We emphasize that further experiments on samples prepared under widely varying conditions, and with different, independently verified particle sizes, are necessary. These experiments are planned for the future to confirm our interpretation.

Acknowledgments

This work was supported financially by the Netherlands Organization for Scientific Research (NWO—Nederlandse Organisatie voor Wetenschappelijk Onderzoek) project number 047-008-021 and Russian Foundation for Basic Research project number 00-15-96615.

References

[1] Hayashi S and Kanamori H 1982 *Phys. Rev.* B **26** 7079
[2] Canham L T 1990 *Appl. Phys. Lett.* **57** 1046
[3] Lehmann V and Gosele U 1991 *Appl. Phys. Lett.* **58** 856
[4] Koshida N and Koyama H 1992 *Appl. Phys. Lett.* **60** 347
[5] Fowler A B, Fang F F, Howard W E and Stiles P J 1966 *Phys. Rev. Lett.* **16** 901
[6] Fukumi K, Chayachara A, Kadono K, Sakaguchi T, Horino Y, Miya M, Fujii J K, Hayakawa J and Satou M 1994 *J. Appl. Phys.* **75** 3075
[7] Chemla D 1993 *Phys. Today* **46–52**

See endnote 3

[8] Heitmann D and Kotthaus J P 1993 *Phys. Today* **56**
[9] Chang L and Esaki L 1992 *Phys. Today* **36**
[10] Mendez E E (ed) 1993 *Optics of Semiconductor Nanostructures* (Weinheim: VCH)
[11] Mariotto G, Montagna M, Viliani G, Duval E, Lefrant S, Rzepka E and Mai C 1988 *Europhys. Lett.* **6** 239
[12] Ferrari M, Champagnon B and Barland M 1992 *J. Non-Cryst. Solids* **151** 95
[13] Rzepka E, Lefrant S and Taurel L 1979 *Solid State Commun.* **30** 801
[14] Barland M, Duval E, Mai C, Mariotto G, Montagna M and Viliani G 1989 *Physica* A **157** 539
[15] Groote J C, Weerkamp J R W, Seinen J and den Hartog H W 1994 *Phys. Rev.* B **50** 9798
[16] Seinen J, Groote J C, Weerkamp J R W and den Hartog H W 1994 *Phys. Rev.* B **50** 9793
[17] L'vov S G, Cherkasov F G, Vitol A Y and Silaev V A 1996 *Appl. Radiat. Isot.* **47** 1615
[18] Weerkamp J R W, Groote J C, Seinen J and den Hartog H W 1994 *Phys. Rev.* B **50** 9781
[19] Poulet H and Mathieu J-P 1970 *Spectres de Vibration et Symetrie des Cristaux* (Paris: Organization name) See endnote 4
[20] Gilat G and Raubenheimer L 1962 *Phys. Rev.* **144** 390
[21] Stekhanov A and Chisler E 1961 *Fiz. Tverd. Tela* **3** 3514
[22] Bobovich T and Tulub T 1959 *Opt. Spectrosk.* **6** 566
[23] Fujii M, Nagareda T, Hayashi S and Yamamoto K 1991 *Phys. Rev.* B **44** 6243
[24] Duval E 1992 *Phys. Rev.* B **46** 5795
[25] Fermi E and Rasetti F 1931 *Z. Phys.* **71** 689
[26] Gross E and Stekhanov A 1947 *Izv. Akad. Nauk SSR, Ser. Phys.* **11** 364
[27] Kellermann E W 1941 *Proc. R. Soc.* A **178** 17
[28] Bilz H and Kress W 1979 *Phonon Dispersion Relations in Insulators* vol 10 (Berlin: Springer)
[29] Raunio G, Almquist L and Stedman R 1969 *Phys. Rev.* **178** 1496
[30] Shuker R and Gammon R W 1970 *Phys. Rev. Lett.* **25** 222
[31] Duval E, Mariotto G, Montagna M, Pilla O, Viliani G and Barland M 1987 *Europhys. Lett.* **3** 333
[32] Montagna M and Dusi R 1995 *Phys. Rev.* B **52** 10 080
[33] Samsonov G V (ed) 1968 *Handbook of the Physicochemical Properties of the Elements* (New York: Plenum)
[34] Wolf P A 1968 *Proc. Int. Conf. on Light Scattering Spectra of Solids* (New York: Springer) p 273
[35] 1954 *Smithsonian Physical Tables* 9th edn (Washington, DC: Organization name) See endnote 5
[36] Krishnan R S (ed) 1958 *Progress in Crystal Physics* vol 1 (Withwawathan: Organization name)
[37] Smith C, Wilkinson G, Karo A M and Hardy J R 1965 *Lattice Dynamics* (New York: Organization name)
[38] den Hartog H W 1999 *Radiat. Eff. Defects Solids* **150** 167
[39] Vainshtein D I and den Hartog H W 2000 *Radiat. Eff. Defects Solids* **152** 23
[40] Dubinko V I, Turkin A A, Vainshtein D I and den Hartog H W 2000 *J. Nucl. Mater.* **277** 184
[41] Vainshtein D I, Dubinko V I, Turkin A A and den Hartog H W 2000 *Nucl. Instrum. Methods Phys. Res.* B **166–167** 550
[42] Galickii, Kornakov B and Kogan V 1992 *Problems in Quantum Mechanics* (Moscow: Science) See endnote 6
[43] John G C and Singh V A 1995 *Phys. Rep.* **263** 93
[44] John G C and Singh V A 1994 *Phys. Rev.* B **50** 5329

Queries for IOP paper 134075

Journal: **JPhysCM**
Author: **E I Shtyrkov et al**
Short title: **Raman scattering and quantum confinement in heavily electron-irradiated alkali halides**

Page 7

Query 1:
Author: Amended spelling 'Bilz' (as in reference list) OK?

Page 13

Query 2:
Author: Amended wording 'This expression...' OK?

Page 15

Query 3:
Author: [7], [8], [9]: please provide page numbers (and issue Nos if necessary).

Page 16

Query 4:
Author: [19], [35], [36], [37]: please provide names of publishers.

Query 5:
Author: [35]: any editor?

Query 6:
Author: [42]: please supply initial(s) for Galickii.